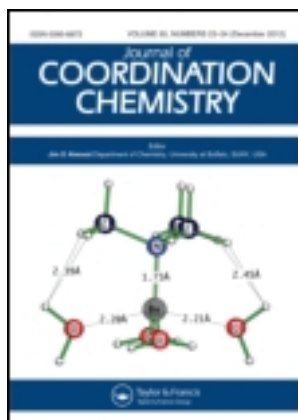


This article was downloaded by: [University of Arizona]

On: 13 December 2012, At: 23:25

Publisher: Taylor & Francis

Informa Ltd Registered in England and Wales Registered Number: 1072954 Registered office: Mortimer House, 37-41 Mortimer Street, London W1T 3JH, UK



Journal of Coordination Chemistry

Publication details, including instructions for authors and subscription information:

<http://www.tandfonline.com/loi/gcoo20>

Syntheses, crystal structures, and properties of Cu(II) and Zn(II) complexes with an asymmetric tripodal ligand

WENWU SUN^{a, b}, QINGRONG CHENG^a, HONG ZHOU^a & ZHIQUAN PAN^a

^a National Engineering Research Center of Phosphate Resources Development and Utilization Wuhan Institute of Technology, Wuhan, P.R. China

^b State Key Laboratory of Phytochemistry and Plant Resources in West China, Kunming Institute of Botany, Chinese Academy of Sciences, Kunming, P.R. China

Accepted author version posted online: 06 Nov 2012. Version of record first published: 12 Dec 2012.

To cite this article: WENWU SUN, QINGRONG CHENG, HONG ZHOU & ZHIQUAN PAN (2013): Syntheses, crystal structures, and properties of Cu(II) and Zn(II) complexes with an asymmetric tripodal ligand, *Journal of Coordination Chemistry*, 66:1, 56-65

To link to this article: <http://dx.doi.org/10.1080/00958972.2012.746459>

PLEASE SCROLL DOWN FOR ARTICLE

Full terms and conditions of use: <http://www.tandfonline.com/page/terms-and-conditions>

This article may be used for research, teaching, and private study purposes. Any substantial or systematic reproduction, redistribution, reselling, loan, sub-licensing, systematic supply, or distribution in any form to anyone is expressly forbidden.

The publisher does not give any warranty express or implied or make any representation that the contents will be complete or accurate or up to date. The accuracy of any instructions, formulae, and drug doses should be independently verified with primary sources. The publisher shall not be liable for any loss, actions, claims, proceedings,

demand, or costs or damages whatsoever or howsoever caused arising directly or indirectly in connection with or arising out of the use of this material.

Syntheses, crystal structures, and properties of Cu(II) and Zn(II) complexes with an asymmetric tripodal ligand

WENWU SUN^{A,B}, QINGRONG CHENG^A, HONG ZHOU^{A*} and ZHIQUAN PAN^{A*}

^aNational Engineering Research Center of Phosphate Resources Development and Utilization, Wuhan Institute of Technology, Wuhan, P.R. China; ^bState Key Laboratory of Phytochemistry and Plant Resources in West China, Kunming Institute of Botany, Chinese Academy of Sciences, Kunming, P.R. China

(Received 29 May 2012; final version received 3 October 2012)

[Cu₂L₂](ClO₄)₂ (**1**) and [Zn₂L₂](ClO₄)₂ (**2**) (HL = 2-[bis(3-aminopropyl)amino]propanol) have been synthesized and characterized. X-ray crystallography analyses show that both are dinuclear with bis-μ-alkoxy-bridged structures. Their molecular structures are centro-symmetric. Each metal adopts a trigonal bipyramidal coordination. Cyclic voltammetry indicates that **1** undergoes two irreversible redox processes with big potential differences ($E_{pa}-E_{pc}$) and ratio of i_{pa}/i_{pc} , while only one reduction peak is observed in **2**. Magnetic susceptibility shows that there is a strong antiferromagnetic interaction ($J = -69.4(4) \text{ cm}^{-1}$) between the two copper(II) centers in **1**. Hydrolysis activities toward 4-nitrophenyl acetate of the two complexes have been investigated and second-order rate constants of **1** and **2** are $(4.3 \pm 0.3) \times 10^{-2}$ and $(3.1 \pm 0.2) \times 10^{-2} \text{ M}^{-1} \text{ s}^{-1}$ in 10% (v/v) CH₃CN aqueous solution at 25 °C.

Keywords: Dinuclear Cu(II) and Zn(II) complexes; Crystal structure; Electrochemistry; Magnetic property; Hydrolysis activity

1. Introduction

Modeling studies on metalloenzymes have been explored for application in medicine and industry and to understand the mechanism of metalloenzymes in biological systems [1]. Research on hydrolytic mechanisms of the natural hydrolysis enzymes shows that attack of nucleophiles to electrophilic substrates is the key process [2]. Kinetics of ZnL-promoted 4-nitrophenyl acetate (NA) hydrolysis shows that Zn(II)-bound alkoxide can generate a strong nucleophilic attack toward carboxy ester, which is responsible for higher hydrolysis activity of complexes [3]. Alkoxy-bridged complexes with N₃O₂ coordination have higher hydrolysis activities, which vary with the structural difference [4]. Some tripodal ligands having N₃O coordination with N(R-NH₂)₂(R-OH) (where R=CH₂CH₂ or CH₂CH₂CH₂) have been synthesized and characterized [5]; however, few studies of hydrolysis activity mimics or physical chemistry properties of this kind of complexes were reported [4a, 5]. There is still a challenge to synthesize small molecules having high activity of metalloenzymes and to reveal the effect of structure on the hydrolysis activities of model compounds [6].

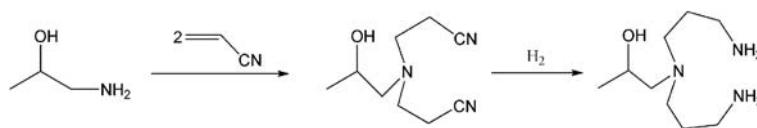
*Corresponding authors. Email addresses: hzhouh@126.com (H. Zhou); zhiqpan@163.com (Z. Pan)

To explore the effect of tripodal ligands and metal ions on the structures and properties of such complexes, we prepared two new dinuclear Cu(II) and Zn(II) complexes using 2-[bis(3-aminopropyl)amino]propanol as tripodal ligands, Scheme 1. Herein, the syntheses, crystal structures, electrochemical properties, magnetic properties and hydrolysis activities toward NA of **1** and **2** are reported.

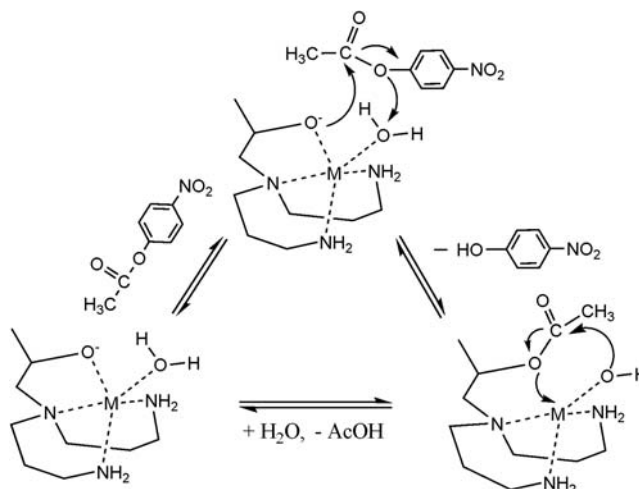
2. Experimental

2.1. Materials and measurements

All solvents and chemicals were of analytical grade and used as received, except methanol that was purified to anhydrous by general method. Elemental analyses were obtained on a Perkin-Elmer 240 analyzer. Cyclic voltammograms were recorded on a CHI 750B electrochemical analyzer, and the measurements were taken in H₂O solutions (5×10^{-4} mol dm⁻³) of the complex containing 0.1 mol dm⁻³ tetraethylammonium perchlorate as the supporting electrolyte. A three-electrode cell equipped with a glass carbon working electrode, a platinum wire as the auxiliary electrode and a saturated calomel electrode as the reference were used. Scanning rates were 100 mVs⁻¹. The solution was deaerated for 15 min before measuring. Magnetic susceptibility of a crystalline-powdered sample was measured on a Quantum Design MPMS-XL SQUID magnetometer from 2.0 to 300 K and the diamagnetic corrections were made according to Pascal's constants.



Scheme 1. Preparation of the tripodal ligand.



Scheme 2. Proposed catalytic mechanism.

2.2. Synthesis of $[\text{Cu}_2\text{L}_2]2\text{ClO}_4$ (1)

2-[Bis(3-aminopropyl)amino]propanol was prepared by our previous method [7]. Yield, 72%. ^1H NMR (D_2O , TMS as reference): δ 0.941 (d, 3H, CH_3C), 1.380 (m, 4H, CH_2), 2.315 (m, 10H, CH_2), 3.742 (m, 1H, CH), 4.664 (d, 1H, OH). Anal. Calc. for $\text{C}_9\text{H}_{27}\text{N}_3\text{O}_3$: C, 48.0; H, 12.1; N, 18.6. Found: C, 48.4; H, 12.5; N, 18.3.

Anhydrous methanol (15 mL) solution of 2-[bis(3-aminopropyl)amino]propanol (0.094 g, 0.5 mmol) was added dropwise to anhydrous methanol solution (10 mL) of $\text{Cu}(\text{ClO}_4)_2 \cdot 6\text{H}_2\text{O}$ (0.186 g, 0.5 mmol). The mixture was stirred for 24 h at room temperature and filtered with blue-green block crystals of $[\text{Cu}_2\text{L}_2] \cdot 2\text{ClO}_4$ suitable for X-ray diffraction obtained by slow evaporation of the resulting filtrate for several days at ambient temperature. Yield, 61%. Anal. Calc. for $\text{C}_{18}\text{H}_{44}\text{N}_6\text{Cl}_2\text{Cu}_2\text{O}_{10}$: C, 30.8; H, 6.3; N, 12.0. Found: C, 31.2; H, 6.2; N, 11.9. IR (KBr, cm^{-1}): 3284, 3321 (N–H), 3456 (O–H), 1096 (ClO_4^-).

2.3. Synthesis of $[\text{Zn}_2\text{L}_2]2\text{ClO}_4$ (2)

This compound was prepared by a similar procedure as described above, except that $\text{Zn}(\text{ClO}_4)_2 \cdot 6\text{H}_2\text{O}$ was used instead of $\text{Cu}(\text{ClO}_4)_2 \cdot 6\text{H}_2\text{O}$. The obtained crystals suitable for X-ray diffraction are colorless prisms. Yield, 53%. Anal. Calc. for $\text{C}_{18}\text{H}_{44}\text{N}_6\text{Cl}_2\text{Zn}_2\text{O}_{10}$: C, 30.6; H, 6.3; N, 11.9. Found: C, 30.9; H, 6.2; N, 12.1. IR (KBr, cm^{-1}): 3289, 3329 (N–H), 3449 (O–H), 1095 (ClO_4^-). *Caution:* Although no problem was encountered in this work, transition metal perchlorates are potentially explosive and should be handled in small quantities.

2.4. X-ray crystallography

Diffraction intensity data were collected on a SMART-CCD area-detector diffractometer at 293 K using graphite monochromated Mo K_α radiation ($\lambda = 0.71073 \text{ \AA}$). Data reduction and cell refinement were performed by SMART and SAINT [8]. The structures were solved by direct methods (Bruker SHELXTL) and refined on F^2 by full-matrix least squares (Bruker SHELXTL) using all unique data [9]. The non-H atoms in the structure were treated as anisotropic. Hydrogens were located geometrically and refined in riding mode.

2.5. Kinetic studies

Catalytic hydrolysis rates of NA by the complexes were measured by a similar method described in the literature [5]. Buffer solution containing 20 mM Tris–HCl (pH 6.8–8.8) was used and the ionic strength was adjusted to 0.1 mol L^{-1} with NaNO_3 solution. NA and the complexes were mixed in the buffer solution and release of 4-nitrophenolate in 10% CH_3CN (v/v) aqueous solution at 25°C was recorded by UV-2450 spectrophotometer. [NA] was set to be constant, and the observed first-order rate constant k_{obsd} (s^{-1}) was measured in the presence of various concentrations of $[\text{M}_2\text{L}_2]^{2+}$ (1–3 mM). The k_{obsd} was calculated from the decay slope (4-nitrophenolate release rate/[NP]). The second-order rate constant for NA hydrolysis was calculated from $k_{\text{obsd}}/[\text{complex}]_{\text{total}}$ [4a].

3. Results and discussion

3.1. Synthesis and spectral properties

A blue-green dinuclear copper(II) complex and a colorless dinuclear zinc(II) complex were obtained by reaction of 2-[bis(3-aminopropyl)amino]propanol and $M(\text{ClO}_4)_2 \cdot 6\text{H}_2\text{O}$ ($M=\text{Cu}$ or Zn) in methanol solution. In the IR spectrum of **1**, signals at 3284 and 3321 cm^{-1} are assigned to the N–H stretch. The presence of a broad band at 3456 cm^{-1} is characteristic of OH groups [5a]. A symmetrical band at 1096 cm^{-1} indicates the presence of uncoordinated perchlorate [10]. The IR spectrum of **2** is similar to that of **1**, and assignments for the characteristic vibrations of **2** are the same as for **1**.

3.2. Description of the crystal structure

Perspective views of the molecular structures for **1** and **2** are shown in figure 1 with atom numbering scheme. Crystallographic data and details about the data collection are presented in table 1. Selected bond distances and angles relative to copper(II) and zinc(II) coordination spheres are listed in table 2.

3.2.1. Crystal structure of 1. The crystal structure of **1** consists of $[\text{Cu}_2\text{L}]^{2+}$ and two non-coordinated perchlorates. The molecular structure is centrosymmetric in which the center is located at the middle of two Cu(II) ions. The Cu(II) ions are connected by two μ_2 -hydroxypropane-bridged groups with Cu–Cu distance of 2.969(1) Å and Cu(1)–O(1)–Cu

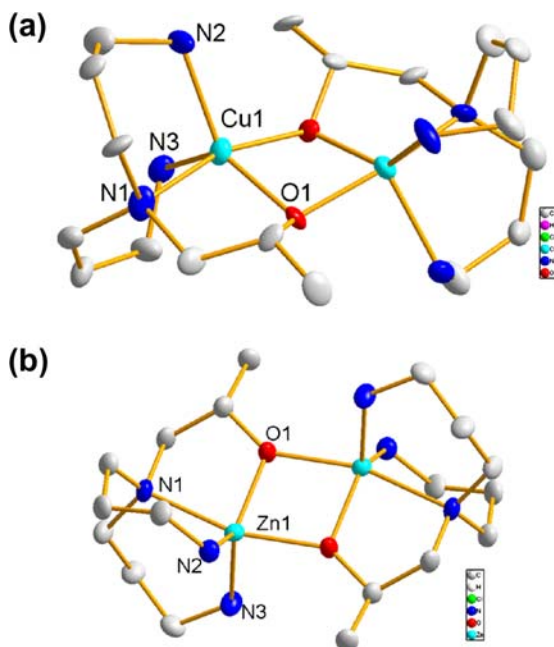


Figure 1. Structural depiction of **1**(a) and **2**(b).

Table 1. Crystal data and structure refinement for **1**.

Empirical formula	C ₁₈ H ₄₄ Cl ₂ Cu ₂ N ₆ O ₁₀	C ₁₈ H ₄₄ Cl ₂ N ₆ O ₁₀ Zn
Formula weight	702.57	706.23
Crystal system	Orthorhombic	Monoclinic
Space group	Pnn2	P2(1)/n
<i>a</i> , <i>b</i> , <i>c</i> (Å)	11.859(3), 13.311(3), 9.273(2)	7.9671(6), 15.2489(12), 2.1407(10)
α, β, γ(°)	90.00, 90.00, 90.00	90.00, 98.15, 90.00
Volume (Å ³)	1463.8(6)	1460.2(2)
<i>Z</i> , <i>D</i> _{calc} (g/cm ³)	2, 1.594	2, 1.606
μ (Mo-Kα) (mm), <i>F</i> (0 0 0)	1.693, 732	1.884, 736
Crystal size (mm)	0.20 × 0.22 × 0.26	0.20 × 0.22 × 0.26
Temperature (K)	291	291
Mo Kα radiation (Å)	0.71073	0.71073
θ Range (°)	2.3–26.0	2.2–26.0
Data set	−14 ≤ <i>h</i> ≤ 14; −12 ≤ <i>k</i> ≤ 16; −11 ≤ <i>l</i> ≤ 10	−9 ≤ <i>h</i> ≤ 6; −18 ≤ <i>k</i> ≤ 18; −14 ≤ <i>l</i> ≤ 14
Total, uniq. data <i>R</i> (int)	8058, 2716, 0.055	8268, 2852, 0.040
Observed data [<i>I</i> > 2.0 sigma(<i>I</i>)]	2130	2369
<i>N</i> _{ref} , <i>N</i> _{par}	2716, 173	2852, 173
<i>R</i> , <i>wR</i> ₂ , <i>S</i>	0.0558, 0.1203, 1.01	0.0474, 0.1091, 1.03
Max. and av. shift/error	0.00, 0.00	0.00, 0.00
Min. and max. resd. dens. (e/Å ³)	−0.60, 0.38	−0.66, 0.30

Table 2. Selected structural data for **1** and **2**.

1		2	
Bond	Length (Å)	Bond	Length (Å)
Cu1–O1 ⁱ	1.914(4)	Zn1–O1 ⁱ	2.089(3)
Cu1–O1	1.975(4)	Zn1–O1	1.958(3)
Cu1–N1	2.048(5)	Zn1–N1	2.232(3)
Cu1–N2	2.105(7)	Zn1–N2	2.042(3)
Cu1–N3	2.122(7)	Zn1–N3	2.054(3)
Bond angles	Values (°)	Bond angles	Values (°)
O1–Cu1–O1 ⁱ	76.71(18)	O1–Zn1–N1	82.91(12)
O1–Cu1–N1	87.92(18)	O1–Zn1–N2	122.32(13)
O1–Cu1–N2	137.0(3)	N1–Zn1–N2	96.53(13)
N1–Cu1–N2	96.4(3)	O1–Zn1–N3	119.43(15)
O1–Cu1–N3	126.9(2)	N1–Zn1–N3	94.3(3)

(1) angle of 99.52(1)°, comparable to those of similar binuclear Cu(II) complexes of this type [5b]. Each Cu(II) is trigonal bipyramidal with the basal plane composed of two primary amine nitrogens N2 and N3 and a bridging hydroxypropane oxygen O1; the apical positions are occupied by a tertiary nitrogen N1 and the other bridging hydroxypropane oxygen O1. The angle of N1–Cu1–O1 is 97.92(1)°. The average distances are Cu–O 1.945 Å and Cu–N 2.099 Å, which are very close to similar ones in a hydroxyethyl-bridged dinuclear copper(II) complex [5b]. The mean plane deviation of the plane consisting of two copper(II) and two bridged hydroxypropane oxygens is 0.174(3) Å, indicating that the four atoms are located in a distorted plane.

Perchlorates in the lattice join adjacent dinuclear units by hydrogen bonds to form a saddle configuration, where each perchlorate is a hydrogen bond acceptor to three dinuclear units through C–H–O and N–H–O (figure 2). The relative parameters are listed in table 3.

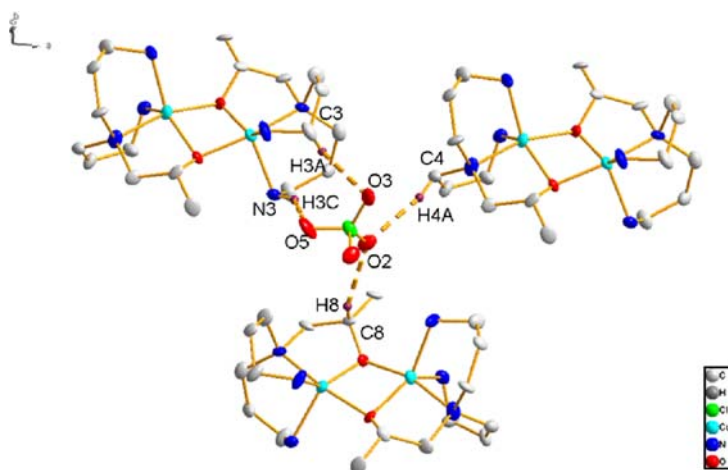


Figure 2. View of the hydrogen bonded interactions between one perchlorate with three $[\text{Cu}_2\text{L}]^{2+}$ groups in **1**.

3.2.2. Crystal structure of 2. Except for different metal ions, Cu for **1**, and Zn for **2**, **1** and **2** have the same composition and similar coordination, figure 1(b). In **2**, Zn–Zn separation is 3.106(9) Å, and Zn(1)–O(1)–Zn(1) angle is 100.16(11)°, slightly larger than in **1**. The coordination number, polyhedron and composition related to the coordination environment of the metal ions are the same. The Zn–N and Zn–O distances are in the range of similar complexes [11]. The stacking pattern of **2** (figure 3) shows that oxygens of each perchlorate anion have hydrogen bonding interactions with three adjacent cations, similar to that of **1**. The hydrogen bonds involve C–H–O and N–H–O, and relative parameters are listed in table 3.

3.3. Electrochemical studies

Electrochemical properties of **1** and **2** have been studied by cyclic voltammetry in distilled water containing 0.1 M KCl. Typical cyclic voltammograms of **1** and **2** are given in Supplementary material. For **1**, when scanning from 0.5 to -1.2 V at a scan rate of 0.1 V s^{-1} , there are two anodic peaks ($E_{\text{pa}1} = 0.053$ V and $E_{\text{pa}2} = 0.262$ V) and cathodic peaks ($E_{\text{pc}1} = -0.658$ V and $E_{\text{pc}2} = -0.260$ V). The separations of the anodic and cathodic

Table 3. Hydrogen bonds parameters for **1** and **2**.

	D–H...A	d(H–A)	D(D–A)	∠DHA
1	N3–H3C...O5	2.4700	3.226(9)	142.00
	C3–H3A...O3	2.5900	3.052(10)	110.00
	C4–H4A...O2	2.4600	3.417(10)	168.00
	C8–H8A...O2	2.4900	3.331(9)	144.00
2	N2–H2C...O3	2.2300	3.100(4)	163.00
	N2–H2D...O2	2.2400	3.124(4)	166.00
	N3–H3C...O5	2.3200	3.184(4)	162.00
	C4–H4A...O4	2.5000	3.435(5)	162.00
	C9–H9C...O2	2.5800	3.443(6)	150.00

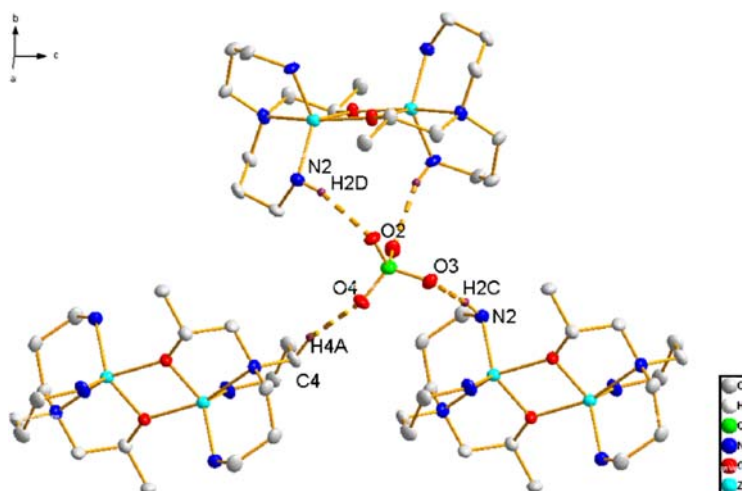


Figure 3. View of the hydrogen bond interactions between $[\text{Zn}_2\text{L}]^{2+}$ and a perchlorate in **2**.

peak potential of 711 and 522 mV, respectively, and the ratio of anodic to cathodic peak currents, $i_{\text{pa}}/i_{\text{pc}}=2.5$, indicate that redox processes are irreversible [10a]. The irreversibility of the redox process can be contributed to instability of Cu(I) within the strong ligand field generated by the alkoxide and amine [11].

The cyclic voltammogram of **2** was obtained by the same experimental conditions. The electrochemical behavior of **2** (Supplementary Material) is quite different from that of **1**. Considering that the complexes have same ligands with same coordination composition, the difference of electrochemical properties can be assigned to the different metal ions in the complexes. When scanning from 1.0 to -1.2 V at a scan rate of 100 mV s^{-1} , only one reduction process was observed at $E_{\text{pc}}=-0.668$ V; no oxidant wave was found when rescanned, indicating an irreversible electrode process, in agreement with the results of similar dinuclear Zn(II) complexes [5a].

3.4. Magnetochemistry

The temperature dependence of the magnetic susceptibility of **1** from 2.0 to 300 K is shown in figure 4 in the form of $\chi_m T$ vs. T . The $\chi_m T$ value gradually decreases with decline of temperature, indicating the presence of antiferromagnetic interaction between copper(II) ions in the complex. The magnetic susceptibility is fit by an expression given in equation (1), which is based on the general isotropic exchange ($\hat{H}=-2J\hat{S}_1\cdot\hat{S}_2$), with $S_1=S_2=1/2$ [12].

$$\chi_m = \frac{2Ng^2\beta^2}{kT} \times \frac{1}{3 + e^{-2J/kT}} \quad (1)$$

χ_m is the paramagnetic susceptibility, g is the average gyromagnetic ratio; the other symbols have their usual meanings. The best set of parameters obtained for **1** by using the above model is as follows: $J=-69.4$ (4) cm^{-1} , $g=2.00$ (0) with a coefficient of determination of $R=4 \times 10^{-5}$. The J value is very close to those of other dinuclear copper(II)

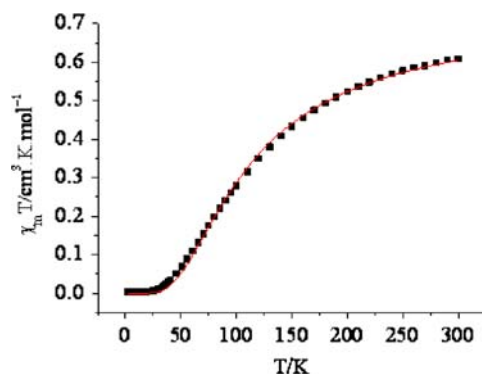


Figure 4. Experimental and calculated plots of $\chi_m T$ vs. T . The solid line shows the best fit with equation (1).

complexes, suggesting a strong antiferromagnetic interaction between the two copper(II) centers [13]. However, the magnetic interactions in **1** are much smaller than those of our previous reported macrocyclic dinuclear copper(II) complexes [12, 14]. Considering that the Cu–Cu distance in **1** is very close to those of the macrocyclic complexes, the magnetic difference can be mainly assigned to the magnetic pathway. For the macrocyclic complexes, copper and two bridged phenoxides are almost in one plane, leading to effective overlap for the magnetic interactions, while in **1**, the bridged oxygens and two copper (II) ions are in a distorted plane, decreasing the magnetic interactions due to less overlap of the magnetic pathway.

3.5. NA hydrolysis promoted by $[\text{Cu}_2\text{L}_2](\text{ClO}_4)_2$ and $[\text{Zn}_2\text{L}_2](\text{ClO}_4)_2$

Reactivity of the two complexes toward hydrolysis of phosphomonoesters or carboxy ester has also been investigated. Since no obvious hydrolysis activity of the phosphomonoesters promoted by the two complexes was observed, the hydrolytic cleavage of NA by the complexes is reported herein. The activity has been investigated by monitoring the hydrolysis of NA promoted by $[\text{Cu}_2\text{L}_2](\text{ClO}_4)_2$ and $[\text{Zn}_2\text{L}_2](\text{ClO}_4)_2$ at different concentrations (1.0–3.0 mM) in the pH range 6.7–8.8. The dependence of observed pseudo-first-order rate constants (k_{obs}) for hydrolysis of NA on pH and on total concentration of the complexes are shown in Supplementary Material and figure 5. The results show that k_{obs} increases with pH, and k_{obs} is almost unchanged when pH is larger than 8.5 with maximum k_{obs} at pH=8.8. So, pH of 8.8 was chosen to conduct hydrolysis measurements. The second-order rate constant K_{NA} for **1** and **2** is $(4.3 \pm 0.3) \times 10^{-2}$ and $(3.1 \pm 0.2) \times 10^{-2} \text{ M}^{-1} \text{ s}^{-1}$, calculated from the slope of the straight line k_{obs} vs. [complex]. The constants of **1** and **2** are 2.1 and 1.47 times greater than that of a double hydroxyethyl-bridged dizinc complex [4b], but lower than those of the corresponding Zn(II)-bound alkoxide complexes [3b, 4a, 15]. According to the literature [4a], hydrolysis activity of the double alkoxide-bridged complexes is from cleavage of the bridged-alkoxide followed by binding of OH^- to form the active species, which is affected by the stability of the double alkoxide-bridged structures in the complexes. **1** and **2** contain two 3-aminopropyl moieties in their structure, which is more flexible than two 2-aminoethyl moieties in zinc(II) 2-[bis(2-aminoethyl)amino]ethanol complex (**3**). The more flexible structures of **1** and **2** make them more

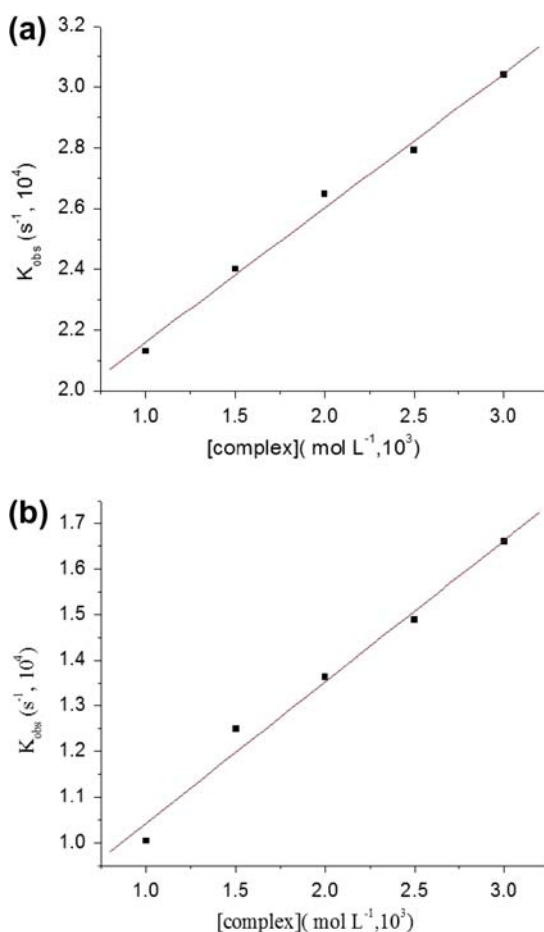


Figure 5. Dependence of k_{obs} on total concentration of the complexes at pH 8.8 with ionic strength 0.1 M (NaNO_3) in the presence of 10% (v/v) CH_3CN , correlation coefficient >0.99 . The effect of the spontaneous hydrolysis for buffer solution has been eliminated. (a) for **1** and (b) for **2**.

stable than **3**, and the steric hindrance caused by CH_3 in **1** and **2** also hinders the binding of OH^- , therefore, the hydrolysis activities of **1** and **2** are smaller than that of **3** having similar structure with **1** and **2**. The suggested catalytic mechanism of the complexes is shown in Scheme 2. The deprotonated hydroxypropyl pendants can nucleophilically attack acyl carbon of NA, while a hydrogen of water bound to the metal ion acts as a receptor for the leaving group, 4-nitrophenol anion. Then the metal-bound hydroxide is a nucleophile to attack the “acyl” to recycle the hydrolysis [3a].

4. Conclusion

The reaction of 2-[bis(3-aminopropyl)amino]propanol and $\text{M}(\text{ClO}_4)_2 \cdot 6\text{H}_2\text{O}$ ($\text{M}=\text{Cu}$ or Zn) in methanol gives two hydroxypropane-bridged dinuclear complexes. Except for the difference of metal ions, the two complexes have same coordination number, polyhedron and

composition as well as similar hydrogen-bonding interactions between the cations of the complexes and perchlorate anions. Due to the difference of metal ions in the complexes, they have different electrochemical behavior. The magnetic interaction in **1** shows that hydroxypropane-bridged dicopper(II) complex has strong antiferromagnetic interactions, but the magnitude is smaller than those of phenoxide-bridged dicopper complexes. The two complexes have hydrolysis activities toward NA.

Supplementary data

Full lists of crystallographic data have been deposited with the CCDC as file numbers CCDC 880852 for **1** and 880853 for **2**.

Acknowledgements

We are thankful for the financial support from the National Nature Science Foundation of China (21171135, 20971102 and 20871097).

References

- [1] (a) T. Böttcher, S.A. Sieber. *J. Am. Chem. Soc.*, **132**, 6964 (2010). (b) M.D. Bednarski, H.K. Chenault, S. Simon, G.M. Whitesides. *J. Am. Chem. Soc.*, **109**, 1283 (1987). (c) K.D. Cramer, S.C. Zimmerman. *J. Am. Chem. Soc.*, **112**, 3680 (1990).
- [2] (a) S. Parimala, M. Kandaswamy. *Inorg. Chem. Commun.*, **6**, 1252 (2003). (b) M. Yamami, H. Furutachi, T. Yokoyama, H. Ōkawa. *Inorg. Chem.*, **37**, 6832 (1998). (c) E. Kimura, T. Shiota, T. Koike, M. Shire, M. Kodama. *J. Am. Chem. Soc.*, **112**, 5805 (1990).
- [3] (a) S.A. Li, J. Xia, D.X. Yang, Y. Xu, D.F. Li, M.F. Wu, W.X. Tang. *Inorg. Chem.*, **41**, 1807 (2002). (b) E. Kimura, I. Nakamura, T. Koike, M. Shionoya, Y. Kodama, T. Ikeda, M. Shirot. *J. Am. Chem. Soc.*, **116**, 4764 (1994).
- [4] (a) J. Xia, Y. Xu, S.A. Li, W.Y. Sun, K.B. Yu, W.X. Tang. *Inorg. Chem.*, **40**, 2394 (2001). (b) S.A. Li, D.F. Li, D.X. Yang, J. Huang, Y. Xu, W.X. Tang. *Inorg. Chem. Commun.*, **6**, 221 (2003).
- [5] (a) F.E. Hahn, C. Jocher, T. Lügger, T. Pape. *Z. Anorg. Allg. Chem.*, **629**, 2341 (2003). (b) N.F. Curtis, O.P. Gladkikh, S.L. Heath, K.R. Morgan. *Inorg. Chim. Acta*, **348**, 242 (2003).
- [6] M. Thirumavalavan, P. Akilan, M. Kandaswamy. *Polyhedron*, **25**, 2623 (2006).
- [7] H. Zhou, L. Chen, R. Chen, Z.H. Peng, Y. Song, Z.Q. Pan, Q.M. Huang, Z.W. Bai. *CrystEngComm*, **11**, 671 (2009).
- [8] Smart and Saint. *Area Detector Control and Integration Software*, Madison, WI (1996).
- [9] G.M. Sheldrick. *SHELXTL V5.1 Software Reference Manual*, Bruker AXS, Inc., Madison, WI (1997).
- [10] (a) T.M. Rajendiran, R. Venkatesan, P. Sambasiva Rao, M. Kandaswamy. *Polyhedron*, **17**, 3427 (1998). (b) P. Akilan, M. Thirumavalavan, M. Kandaswamy. *Polyhedron*, **22**, 1407 (2003).
- [11] C. Jocher, T. Pape, W.W. Seidel, P. Gamez, J. Reedijk, F.E. Hahn. *Eur. J. Inorg. Chem.*, **24**, 4914 (2005).
- [12] J. Pan, L. Cheng, H. Zhou, Z.Q. Pan, Q.M. Huang, X.L. Hu. *Polyhedron*, **29**, 1588 (2010).
- [13] (a) M. Kandaswamy, P. Suthakaran, V. Murugan, Babu Varghese. *J. Inorg. Biochem.*, **103**, 401 (2009). (b) F. Hasanvand, Z. Golyrostomi, S.M. Ghattali, S. Amani. *Arch. Appl. Sci. Res.*, **1**, 142 (2009).
- [14] Q.R. Cheng, H. Zhou, Z.Q. Pan, J.Z. Chen. *Polyhedron*, **30**, 1171 (2011).
- [15] C. Bazzicalupi, A. Bencini, E. Berni, A. Bianchi, V. Fedi, V. Fusi, C. Giorgi, B. Valtancoli. *Inorg. Chem.*, **38**, 4115 (1999).